

Rolling structure from bilayer nanofilm by mismatch

Jian-Gang Li(李建刚), Xiao-Pi Geng(耿小丕), Qian-Nan Gao(高倩男), Jun Zhu(朱俊), Zhi-Xiang Gao(高志翔), and Hong-Wei Zhu(朱弘伟)

Citation: Chin. Phys. B, 2023, 32 (**12**): 126201. DOI: 10.1088/1674-1056/ace032
Journal homepage: http://cpb.iphy.ac.cn; http://iopscience.iop.org/cpb

What follows is a list of articles you may be interested in

Fast prediction of the mechanical response for layered pavement under instantaneous large impact based on random forest regression

Ming-Jun Li(励明君), Lina Yang(杨哩娜), Deng Wang(王登), Si-Yi Wang(王斯艺), Jing-Nan Tang(唐静楠), Yi Jiang(姜毅), and Jie Chen(陈杰)

Chin. Phys. B, 2023, 32 (**4**): 046203. DOI: 10.1088/1674-1056/acb76a

Analytical determination of non-local parameter value to investigate the axial buckling of nanoshells affected by the passing nanofluids and their velocities considering various modified cylindrical shell theories

Soheil Oveissi, Aazam Ghassemi, Mehdi Salehi, S. Ali Eftekhari, and Saeed Ziaei-Rad

Chin. Phys. B, 2023, 32 (**4**): 046201. DOI: 10.1088/1674-1056/ac9cba

Molecular dynamics study of coupled layer thickness and strain rate effect on tensile behaviors of Ti/Ni multilayered nanowires

Meng-Jia Su(宿梦嘉), Qiong Deng(邓琼), Lan-Ting Liu(刘兰亭), Lian-Yang Chen(陈连阳), Meng-Long Su(宿梦龙), and Min-Rong An(安敏荣)

Chin. Phys. B, 2021, 30 (**9**): 096201. DOI: 10.1088/1674-1056/abf10a

High-pressure elastic anisotropy and superconductivity of hafnium: A first-principles calculation

Cheng-Bin Zhang(张成斌), Wei-Dong Li(李卫东), Ping Zhang(张平), and Bao-Tian Wang(王保田)

Chin. Phys. B, 2021, 30 (**5**): 056202. DOI: 10.1088/1674-1056/abd6f6

Giant magnetic moment at open ends of multiwalled carbon nanotubes

Wang Gang (王钢), Chen Min-Jiang (陈闽江), Yu Fang (余芳), Xue Lei-Jiang (薛磊江), Deng Ya (邓娅), Zhang Jian (张键), Qi Xiao-Ying (齐笑迎), Gao Yan (高燕), Chu Wei-Guo (褚卫国), Liu Guang-Tong (刘广同), Yang Hai-Fang (杨海方), Gu Chang-Zhi (顾长志), Sun Lian-Feng (孙连峰)

Chin. Phys. B, 2015, 24 (**1**): 016202. DOI: 10.1088/1674-1056/24/1/016202

Rolling structure from bilayer nanofilm by mismatch

Jian-Gang Li(李建刚)[1,†], Xiao-Pi Geng(耿小丕)[2], Qian-Nan Gao(高倩男)[2], Jun Zhu(朱俊)[3], Zhi-Xiang Gao(高志翔)[1], and Hong-Wei Zhu(朱弘伟)[1]

[1] *School of Physics and Electronic Science, Shanxi Datong University & Shanxi Province Key Laboratory of Microstructure Electromagnetic Functional Materials, Shanxi Datong University, Datong* 037009, *China*
[2] *Department of Mathematics and Physics, Hebei Petroleum University of Technology, Chengde* 067000, *China*
[3] *School of Physical Science and Technology, Inner Mongolia University, Hohhot* 010021, *China*

(Received 13 February 2023; revised manuscript received 2 June 2023; accepted manuscript online 21 June 2023)

A continuum theoretical scheme for self-rolling nanotubes from bilayers by mismatch is obtained by considering surface elasticity, surface stress, and symmetry lowering effects. For an ultrathin nanofilm with only several nanometers in thickness, isotropic mismatch, and isotropic surface stress usually induce anisotropic rolling behavior. The isotropic Timoshenko formula should be modified anisotropically to explain the mechanical behavior of anisotropic rolling structure of nanotubes accurately. The nanofilm rolls up in tangential direction while remaining straight in cylindrical direction theoretically. Therefore, in this paper the anisotropic shape of nanotubes is taken into consideration. Along the cylindrical direction, although it maintains straight and its residual strain is uniform, the stress varies in the radial direction due to the Poisson's effect of tangential strain. The results of the current theory applied to Si–Si nanotube, InAs–GaAs nanotube, and InGaAs–Cr nanotube systems show good agreement with the experimental data. Beside the surface elasticity effect and surface stress effect, the symmetry breaking and the anisotropic rolling structure are of great importance in theoretically describing the mechanical behavior of rolling-up of nanotubes.

Keywords: nanofilms, nanotubes, surface effects, self rolling

PACS: 62.20.–x, 62.20.D–, 68.35.Gy, 81.40.Jj **DOI:** 10.1088/1674-1056/ace032

1. Introduction

Over the past decade, nanostructures have received a great deal of attention.[1,2] They were widely applied to nanoelectromechanical systems (NEMS).[3] Nanostructures, such as nanoparticles,[4] nanobeams,[5,6] nanowires,[7] nanofilms,[8] and nanotubes,[9] are significantly different from bulk structures in mechanics. As important components of NEMS, nanostructures were usually used as nanoactuators,[10] nanosensors,[11] nanoresonators,[12] nanogenerators,[13,14] drug delivery devices,[15] etc. But on the other hand, the small size of nanostructures means large surface-to-volume ratio, which induces the size-dependent property in mechanics.[16–19] The size-dependent and surface-modulated properties in mechanics induce significant difference between nanostructure material and bulk material.[20–22] The applicability of continuous medium mechanics on a nano scale was discussed by Zhao.[23] Cheng[23] improved Thomas–Fermi–Dirac (TFD) model to study the generation mechanism of the residual stress within films. By using Thomas–Fermi–Dirac–Cheng (TFDC) model, the nanotube formation and the corresponding residual stress were studied.[23]

In order to predict the size-dependent elastic properties of nanosized structures theoretically, Gurtin and Murdoch gave a surface elasticity theoretical model.[24] In their theory, the surface slice was considered as an absolutely two-dimensional (2D) slice with elasticity but no thickness. The completely 2D slice with surface elastic coefficient ideally adheres to the bulk-like core of nanofilms. Therefore, their theoretical model is called core–surface model. Miller and Shenoy studied the size-dependent and surface-modulated mechanical behavior of nanofilm by using this core–surface model.[25] In order to develop surface elasticity theory, another theoretical model was established by introducing surface slice thickness, named core–shell model.[26,27] The core–shell model was used to extract nanowire mechanical behavior,[26] nanofilm Young's modulus,[28] and nanofilm self-equilibrium, and self-bending characteristics, etc.[29] There rises a problem in both core–surface model and core–shell model. These two hybrid models divide a nanofilm into surface area and bulk like area. At interface between these two areas, Young's modulus changes suddenly. Although this sudden change was delimited by introducing exponential variation Young's modulus,[30] the Young's modulus derivative's sudden change also exists at interface. In order to eliminate the interface, cylindrical theoretical model was introduced to investigate the bending problem, Young's modulus, Poisson's ratio, etc.[31,32]

Researchers showed that nanofilms can be rolled by surface stress and interface mismatch to form nanotubes.[33] Zhang and Ionov reported self-rolling polyurethane film. The

[†]Corresponding author. E-mail: Lijiangang@sxdtdx.edu.cn; Lijiangang1127@163.com

© 2023 Chinese Physical Society and IOP Publishing Ltd

reversible self-rolling behavior of the bilayer films may allow development of the actuator.[34] Exploiting physical and mechanical properties in rolled-up structures has inspired numerous applications.[35] The research of mechanical self-rolling behavior can promote the development of techniques for manufacturing rolled-up structure.[36] Stoney gave a bending theory about coating.[37] The thinner film thickness was neglected in Stoney theory. Therefore, Stoney formula can work only when film thickness is much less than its substrate thickness. Timoshemko formula introduced film thickness to explain the thermal expansion-induced bending behavior.[38] The bending of bilayer induced by interface mismatch was also explained by Timoshenko formula.[39,40] For a nanofilm with only several nanometers, surface effects are of great importance for film mechanical behavior.[21] Zang and Liu modified Timoshenko formula by considering surface effects.[41] They studied Si–Si nanotube and InAs–GaAs nanotube by using their modified Timoshenko formula. When explaining Si–Si nanotube radius, surface elasticity was chosen as positive. But experimental detection and simulated calculation indicate that Si nanofilm surface elasticity is minus.[19,21] The opposite sign of Si nanofilm surface elastic constant in Ref. [41] needs to be discussed further. Symmetry lowering effect may be a key to solving the surface elastic problem. Cylindrical theoretical model was established to estimate the radius of rolling-up structure.[31] In cylindrical theoretical model, the surface effect and symmetry lowering effect were introduced to modify Timoshenko formula. But the anisotropic rolling structure was missed in Ref. [31]. It is not easy to bend a nanofilm into an isotropic bowl-like object. An ultra-thin nanofilm is usually rolled into a nanotube.[42–44] The formed nanotubes are no longer an isotropic structure as explained by Timoshenko's theory. Cylindrical direction keeps straight and not any bent theoretically. Isotropic Timoshenko formula should be modified anisotropically. Furthermore, cylindrical strain (*i.e.* the strain in cylindrical direction) affects nanotube radius and tangential elongation strain obviously. Therefore, the theory should be established to explain the formation of nanotubes from nanofilms. Surface elasticity, surface stress, symmetry-lowering effects, and anisotropic structure (nanoscroll structure) should be included in the theoretical scheme.

In this paper, a continuum theoretical model for describing self-rolling of strained bilayers is established. The surface elasticity effect, surface stress effect, symmetry-lowering effect, and the anisotropic structure (nanoscroll structure) are considered. The rolling-up nanotube radius, tangential elongation strain, and cylindrical uniform deformation are discussed. Lattice constant, stress, and strain within nanotube wall are also discussed.

2. Theory and models

Since a nanofilm is rolled into a nanotube, the in-plane direction x coordinate is replaced by the tangential direction t coordinate of nanoscroll. The in-plane direction y coordinate is replaced by the cylindrical direction y coordinate of nanoscroll. And the vertical direction z coordinate is replaced by the radial direction r coordinate.

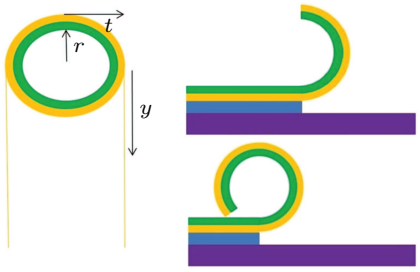


Fig. 1. Schematic representation of the rolled nanotube, with y–t plane fixed at mid-plane of the bilayer system.

In-plane strains along the tangential direction and cylindrical direction of the nanoscroll are denoted as $\varepsilon_{\rm t}$ and ε_y. Radial strain was denoted as $\varepsilon_{\rm r}$. Both $\varepsilon_{\rm t}$ and $\varepsilon_{\rm r}$ are dependent on r coordinate, while ε_y is independent of r coordinate. The reference plane, i.e., $r=0$ is fixed at the mid-plane of the bilayer system, $r=(t_1+t_2)/2$ at the top surface, and $r=-(t_1+t_2)/2$ at the inner surface, with t_1 and t_2 referring to the thickness of nanofilm 1 (inner sublayer) and the thickness of nanofilm 2 (top sublayer), respectively. Experiment demonstrates that the rolled nanotube still holds single crystalline structure, and tangential direction lattice parameters vary linearly in their radial direction.[45] Therefore, tangential strain can be given by[42]

$$\varepsilon_{it}=\varepsilon_{i,0}+\frac{r}{R}=\varepsilon_{i,0}+rk,\quad i=1,2, \tag{1a}$$

$$\varepsilon_{2,0}=\varepsilon_{1,0}+m,\quad \varepsilon_{1,0}=\varepsilon_0\quad i=1,2, \tag{1b}$$

where $k=1/R$ refers to the rolling curvature, R represents the radius of nanoscroll, $\varepsilon_{1\rm t}$ and $\varepsilon_{2\rm t}$ are the tangential strains within nanofilm 1 and nanofilm 2, $\varepsilon_{1,0}$ and $\varepsilon_{2,0}$ are the elongation strains of nanofilm 1 and nanofilm 2, respectively, ε_0 is the elongation of bilayer system, and m is the mismatch between two sub-layers.

The variable quantities to determine nanotube states are ε_0, k, and ε_y. And they need to be determined from relaxation conditions. Radial direction strain $\varepsilon_{\rm r}$ depends on biaxial relaxation since $\sigma_{\rm r}=0$. According to[32]

$$\varepsilon_{\rm r}=-\frac{1}{2}\nu_{\rm b}(\varepsilon_{\rm t}+\varepsilon_y), \tag{2}$$

where $\nu_{\rm b}$ is the effective biaxial Poisson's ratio, and expressed as

$$\nu_{\rm b}=\frac{2c_{11}^{\alpha}+\sqrt{2}c_{12}^{\alpha}-2c_{22}^{\alpha}}{c_{11}^{\alpha}+2\sqrt{2}c_{12}^{\alpha}+2c_{22}^{\alpha}}. \tag{3}$$

For a film under biaxial loading (here, the film is assumed to maintain plane to determine $\nu_{\rm b}$ conveniently), $\sigma_{\rm t}=\sigma_y$ and

$\sigma_r = 0$, one can define this parameter as $v_b = -\varepsilon_r/\varepsilon$, where $\varepsilon = \varepsilon_t = \varepsilon_y$. Elastic constants under cylindrical symmetry are[31,46]

$$\begin{aligned} c_{11}^{\alpha} &= C^{\alpha} + \frac{2}{t}c_{11}^{\alpha,s}, \quad c_{12}^{\alpha} = \frac{2}{t}c_{12}^{\alpha,s}, \\ c_{22}^{\alpha} &= C^{\gamma} + \frac{2}{t}c_{22}^{\alpha,s}, \quad c^{\gamma} = C^{\gamma} + \frac{2}{t}c^{\gamma,s}, \end{aligned} \tag{4}$$

$C^{\alpha} = c_{11} + 2c_{12}$, and $C^{\alpha} = c_{11} - c_{12}$. And then, one only considers the in-plane strains of nanofilms (i.e. cylindrical strain and tangential strain for nanotube condition). According to Ref. [32], the elastic energy density of an isotropic nanofilm can be given by

$$E = \frac{1}{4}Y'(\varepsilon_t + \varepsilon_y)^2 + \frac{1}{4}c^{\gamma}(\varepsilon_t - \varepsilon_y)^2, \tag{5}$$

where Y' is the nanofilm biaxial modulus and given by

$$Y' = 3\frac{c_{11}^{\alpha}c_{22}^{\alpha} - [c_{12}^{\alpha}]^2}{c_{11}^{\alpha} + 2\sqrt{2}c_{12}^{\alpha} + 2c_{22}^{\alpha}}. \tag{6}$$

In order to obtain the elastic energy density which is similar to the counterpart of bulk material, the following Young's modulus and Poisson's ratio are considered in Ref. [32]:

$$Y = \frac{2c^{\gamma}Y'}{Y' + c^{\gamma}}, \tag{7a}$$

$$v = \frac{Y' - c^{\gamma}}{Y' + c^{\gamma}}. \tag{7b}$$

And then, one can obtain the elastic energy density as follows:

$$E = \frac{Y}{2(1-v^2)}\left(\varepsilon_t^2 + \varepsilon_y^2 + 2v\varepsilon_t\varepsilon_y\right). \tag{8}$$

Surface stress on the top surface and inner surface are σ_{ts} and σ_{is}, and strain on the top surface and inner surface are, respectively,

$$\varepsilon_{ts} = \varepsilon_0 + \frac{1}{2}(t_1 + t_2)k + m, \tag{9a}$$

$$\varepsilon_{is} = \varepsilon_0 - \frac{1}{2}(t_1 + t_2)k. \tag{9b}$$

One can obtain the elastic energy density on the top surface and inner surface as follows:[31]

$$\begin{aligned} E_{ts} &= \varepsilon_{ts}\sigma_{ts} + \varepsilon_y\sigma_{ts} + m\sigma_{ts} \\ &= \sigma_{ts}\left[\varepsilon_0 + \frac{1}{2}(t_1 + t_2)k + \varepsilon_y + 2m\right], \end{aligned} \tag{10a}$$

$$\begin{aligned} E_{is} &= \varepsilon_{is}\sigma_{is} + \varepsilon_y\sigma_{is} \\ &= \sigma_{is}\left[\varepsilon_0 - \frac{1}{2}(t_1 + t_2)k + \varepsilon_y\right]. \end{aligned} \tag{10b}$$

Bulk elastic energy density within nanofilm 1 and nanofilm 2 can be given by[31]

$$E_1 = \frac{Y_1}{2(1-v_1^2)}\left[(\varepsilon_0 + zk)^2 + \varepsilon_y^2 + 2v_1(\varepsilon_0 + zk)\varepsilon_y\right], \tag{11a}$$

$$\begin{aligned} E_2 = \frac{Y_2}{2(1-v_2^2)}&\left[(\varepsilon_0 + zk + m)^2 + (\varepsilon_y + m)^2\right. \\ &\left. + 2v_2(\varepsilon_0 + zk + m)(\varepsilon_y + m)\right]. \end{aligned} \tag{11b}$$

It should be mentioned that the basic principle of elastic energy density is the same as that in Ref. [31], but the expression of Eqs. (10) and (11) are different from those in Ref. [31]. This difference is induced by the anisotropic shape of the nanotube. This anisotropy is ignored in Ref. [31].

Total bulk elastic energy can be obtained by integrating bulk elastic energy density in the bilayer system, $-(t_1 + t_2)/2 \le r \le (t_1 + t_2)/2$. Total elastic energy is the sum of bulk elastic energy and surface elastic energy, specifically,

$$\begin{aligned} E_{tot}V &= E_1V_1 + E_2V_2 + E_{ts}A + E_{bs}A \\ &= A\frac{Y_1}{2(1-v_1^2)}\left[\varepsilon_0^2 t_1 + \frac{1}{12}k^2\left(t_1^3 + 3t_1t_2^2\right)\right. \\ &\quad \left. - \varepsilon_0 k t_1 t_2 + \varepsilon_y^2 t_1 + 2v_1\varepsilon_0\varepsilon_y t_1 - v_1 k\varepsilon_y t_1 t_2\right] \\ &\quad + A\frac{Y_2}{2(1-v_2^2)}\left[(\varepsilon_0 + m)^2 t_2 + \frac{1}{12}k^2\left(t_2^3 + 3t_1^2t_2\right)\right. \\ &\quad + (\varepsilon_0 + m)kt_1t_2 + (\varepsilon_y + m)^2 t_2 \\ &\quad \left. + 2v_2(\varepsilon_0 + m)(\varepsilon_y + m)t_2 + v_2k(\varepsilon_y + m)t_1t_2\right] \\ &\quad + A\sigma_{ts}\left[\varepsilon_0 + \frac{1}{2}(t_1 + t_2)k + \varepsilon_y + 2m\right] \\ &\quad + A\sigma_{is}\left[\varepsilon_0 - \frac{1}{2}(t_1 + t_2)k + \varepsilon_y\right], \end{aligned} \tag{12}$$

where V and A are the volume and surface area of the bilayer system (V_1 and V_2 correspond to nanofilm 1 and nanofilm 2, respectively). One can obtain the parameters k and ε_0 from the principle of minimum energy:

$$\frac{\partial E_{tot}}{\partial k} = \frac{\partial E_{tot}}{\partial \varepsilon_0} = 0. \tag{13}$$

They are

$$k = -6\frac{\begin{array}{c}[m(1+v_2) + (v_2 - v_1)\varepsilon_y](t_1 + t_2)\chi t_1 t_2 \\ + \frac{1}{G_1}(1-\chi)t_1t_2(\sigma_{ts} + \sigma_{is}) \\ + \frac{1}{G_1}\left(t_1^2 + t_1t_2 + \chi t_1t_2 + \chi t_2^2\right)(\sigma_{ts} - \sigma_{is})\end{array}}{t_1^4 + 4\chi t_1^3 t_2 + 6\chi t_1^2 t_2^2 + 4\chi t_1 t_2^3 + \chi^2 t_2^4}, \tag{14a}$$

$$\varepsilon_0 = -\frac{\begin{array}{c}\chi\left(t_1^3t_2 + 3t_1^2t_2^2 + 3t_1t_2^3 + \chi t_2^4\right)[m + v_2(\varepsilon_y + m)] \\ + \left\{t_1^4 + 3t_1^3t_2 + 3\chi t_1^2t_2^2 + \chi t_1t_2^3\right\}v_1\varepsilon_y \\ + \frac{1}{G_1}(t_1 + t_2)t_1t_2(1-\chi)(\sigma_{ts} - \sigma_{is}) \\ + \frac{1}{G_1}\left[\left(t_1^3 + 3t_1t_2^2\right) + \chi\left(t_2^3 + 3t_1^2t_2\right)\right](\sigma_{ts} + \sigma_{is})\end{array}}{t_1^4 + 4\chi t_1^3 t_2 + 6\chi t_1^2 t_2^2 + 4\chi t_1 t_2^3 + \chi^2 t_2^4}, \tag{14b}$$

where

$$G_1 = \frac{Y_1}{(1-v_1^2)}, \quad G_2 = \frac{Y_2}{(1-v_2^2)}, \quad \chi = \frac{G_2}{G_1}. \tag{15}$$

Stiffness ratio χ is dependent on size and surface modulated. Equations (14a) and (14b) describe the rolling curvature and

elongation strain in tangential direction, respectively. Elongation strain ε_0 is uniform strain while rolling curvature introduces a gradient of strain. In the cylindrical direction, there is no any rolling (or bending) behavior theoretically. Therefore, cylindrical strain ε_y remains uniform (independent of r coordinate). This anisotropic explanation of nanotubes is different from that of the isotropic Timoshenko formula.[38] Cylindrical strain ε_y affects the nanotube radius and tangential elongation deformation. These effects are described in Eqs. (14a) and (14b). The cylindrical strain ε_y can be taken as a relaxed value (one needs to take the additional condition, i.e., $\partial E_{\rm tot}/\partial\varepsilon_y = 0$). For simplicity, this relaxation can be obtained by uniform deformation (flat condition). Under this condition, there is no difference between tangential direction and cylindrical direction, i.e., $\varepsilon_y = \varepsilon_{\rm t} = \varepsilon$. And then, biaxial strain within the flat appears. Then, the elastic energy density reduces into

$$\begin{aligned} E_{\rm tot}V &= At_1Y_1'\varepsilon^2 + At_2Y_2'(\varepsilon+m)^2 \\ &\quad + 2A\sigma_{\rm ts}(\varepsilon+m) + 2A\sigma_{\rm is}\varepsilon. \end{aligned} \tag{16}$$

The relaxation condition can be obtained by minimizing the free energy of the flat

$$\partial E_{\rm tot}/\partial\varepsilon = 0. \tag{17}$$

The relaxation strain along the cylindrical direction in nanofilm 1 is

$$\varepsilon_y = -\frac{\chi'\gamma m}{(1+\chi'\gamma)} - \frac{1}{t_1Y_1'(1+\chi'\gamma)}(\sigma_{\rm ts}+\sigma_{\rm is}) \tag{18a}$$

and in nanofilm 2 it is

$$\varepsilon_y + m = \frac{m}{(1+\chi'\gamma)} - \frac{1}{t_1Y_1'(1+\chi'\gamma)}(\sigma_{\rm ts}+\sigma_{\rm is}), \tag{18b}$$

where

$$\chi' = Y_2'/Y_1', \tag{19a}$$

$$\gamma = t_2/t_1. \tag{19b}$$

Biaxial modulus ratio χ' is dependent on size and surface modulated. Owing to mismatch at interface, the relaxation cannot be the same in two sub-layers. Nanofilm 2 cylindrical direction relaxation should be $\varepsilon_y + m$ as shown in Eqs. (18a) and (18b).

The constitutive relation of nanofilms can be obtained by using the derivative of elastic energy density

$$\sigma_{\rm t} = \frac{\partial E}{\partial\varepsilon_{\rm t}} = \frac{Y}{(1-\nu^2)}(\varepsilon_{\rm t}+\nu\varepsilon_y), \tag{20a}$$

$$\sigma_y = \frac{\partial E}{\partial\varepsilon_y} = \frac{Y}{(1-\nu^2)}(\varepsilon_y+\nu\varepsilon_{\rm t}). \tag{20b}$$

Owing to straight property, cylindrical strain is identical in each sub-layer and independent of r coordinate. But tangential strain $\varepsilon_{\rm t}$ induces an r-dependent cylindrical stress via Poisson's effect as shown in Eq. (20b).

The relationship between lattice parameter and residual strain is

$$a = a_0(1+\varepsilon) \tag{21a}$$

or

$$\varepsilon = \frac{a-a_0}{a_0}, \tag{21b}$$

where a is the lattice parameter of nanotube wall, a_0 is the initial lattice constant without any strain of nanofilms, and ε is the residual strain within nanotube wall.

3. Results and discussion

If a compressed (stretched) film grows on another film, lattice atom relaxes outward (inward). On the other hand, lattice constants of these two sub-layers are different from each other. The difference in lattice constant induces mismatch at interface. The relaxation (mismatch) exerts two effects on the bilayer system. One is force (stress) effect, which tends to expand (compress) the bilayer system, and the other is torque (moment) effect, which tends to bend the bilayer system. If one film's thickness far outweighs the other film's, the thinner film thickness effect can be neglected, Stoney formula can explain bending behavior well. When the thickness of thinner film is comparable to the that of thicker one, the effect of thinner film thickness influences the bending behavior obviously. For a nanoscaled bilayer system, two sub-layer thickness values are comparable to each other. The bilayer system bending problem induced by interface mismatch cannot be explained by Stoney formula any more. And then, Timoshenko formula, which takes thinner film thickness effect into consideration, came on stage.[38–40] In order to explain the mechanical behavior of nanofilm rolling structures there are still two problems that must be considered. The first problem is surface effect and the corresponding symmetry-lowering effect. The relative number of atoms at surface increases with film thickness decreasing. The atomic environment of surface atoms is different from that of bulk counterpart. Lattice symmetry at surface should also be different from that bulk counterpart. Outside bonding partners are missing, dangling bonds are combined together. The atoms leave from their original equilibrium positions, and then stay in their new equilibrium positions. Lattice structure and interatomic distance are changed. Since elastic constant is very sensitive to the interatomic distance,[26,29] the elastic property is changed. On the other hand, this surface reconstruction expands (or shrinks) the film along in-plane direction and induces reverse relaxation along vertical direction via Poisson's effect. The symmetry of the film is broken and lowered. Therefore, surface elasticity, surface stress and symmetry-lowering effect should be

considered to modify Timoshenko formula. The other problem is the anisotropic structure of nanotubes. For an ultra-thin nanofilm with only several nanometers in thickness, it usually behaves as anisotropic rolling rather than isotropic bending. The isotropic Timoshenko formula should be modified anisotropically. The anisotropic shape of nanotubes should be taken into consideration.

Table 1. Surface elastic constants and surface stress of nanofilms.

Films	$c_{11}^{\alpha,s}$ (N/m)	$c_{22}^{\alpha,s}$ (N/m)	$c_{12}^{\alpha,s}$ (N/m)	$c^{\gamma,s}$ (N/m)	σ_s (N/m)
Strained Si	–15	–5	–38	18	–1.3
Unstrained Si	–15	–5	27	18	–1.1
InAs	40	30	25	25	–1.5
GaAs	20	20	–25	20	–4.5

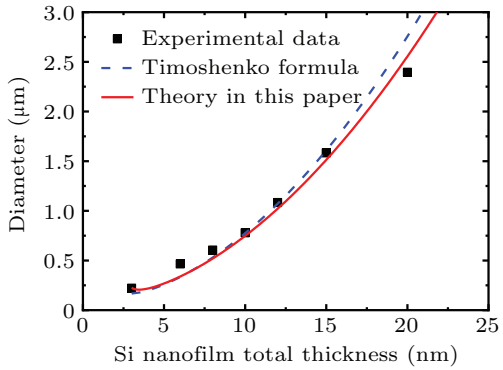


Fig. 2. Curve of diameter of Si/Si tubes versus total thickness of Si film, with strained Si layer thickness fixed at 2 nm and misfit strain m being 2%. The experimental data are cited from Ref. [43].

Making use of the theory given in this work, the rolling behavior of bilayer Si–Si, InAs–GaAs, and InGaAs–Cr nanofilms under isotropic lattice mismatch will be discussed. Figure 2 shows the comparison between the data from the current theory and and experimental results. The experimental results in Fig. 2 are cited from Ref. [43]. The results from our theory (Eq. (14a)) are in good agreement with experimental data as shown in Fig. 2. Bulk elastic constants are $C^{\alpha} = c_{11} + 2c_{12} = 219$ GPa and $C^{\alpha} = c_{11} - c_{12} = 102$ GPa. Surface parameters are listed in Table 1. The surface elastic constants and surface stresses of Si nanofilm are consistent with those from Ref. [19] The results from the classical theory[43] without surface effect are also shown in Fig. 2. Owing to the absence of surface effects, the classical theory does not accord with experiment well. Huang *et al.* studied Si–Si nanotube radius by considering surface stress and surface elasticity effects, showing that the obtained result is in good agreement with experimental results.[40] The fitted surface elastic constant in Ref. [41] is positive. But at the same time, experimental detection and simulated calculation indicate that Si nanofilm surface elasticity is minus.[19,21] The unreasonable positive surface elastic constant in Zang's theory needs further discussing. We suggest that there are two main reasons of this trouble, one is the missing of both lowered symmetry and the corresponding additional elastic constant,[46] and the other is the missing of anisotropic rolling structure. In Ref. [31], lowered symmetry and corresponding additional elastic constant are discussed and all surface constants are negative as indicated by experimental results and simulation results.[19,21] But on the other hand, the value of additional elastic constant $c_{12}^{\alpha,s} = -120$ J·m^{-2} of strained film, cited from Ref. [31], seems to be quite large. Further research about this additional elastic constant indicates its anomalous effect on mechanical property of nanofilm. The larger positive $c_{12}^{\alpha,s}$ drives Young's modulus tends to be smaller and in other words, larger positive $c_{12}^{\alpha,s}$ can soften nanofilm.[32] The abnormal value of additional surface elastic constant, cited in Ref. [31], is induced by the missing of anisotropic rolling structure of nanotubes.

Other important candidates for rolled-up nanotube are InAs–GaAs and InAGaAs–Cr bilayer systems. The InAs–GaAs and InAGaAs–Cr bilayer systems are underestimated by classical Timoshenko formula.[42,48] The experimental data in Figs. 3 and 4 are cited from Refs. [44,47], respectively. Zang and Liu studied the radius of rolled-up nanotube by introducing surface stress effect and surface elasticity effect.[41] The symmetry-lowering effect is introduced to estimate the InAs–GaAs nanotube radius in Ref. [31]. In Ref. [31], the anisotropic rolling structure of nanotubes is missed. In the present work, the surface effect, symmetry-lowering effect, and anisotropic rolling structure are considered to explain the rolling behavior of InAs–GaAs bilayer system and InAGaAs–Cr bilayer system. The bulk Young's moduli and Poisson's ratios, $Y_{\mathrm{InAs}} = 51.42$ GPa, $\nu_{\mathrm{InAs}} = 0.35$, and $Y_{\mathrm{GaAs}} = 85.06$ GPa, $\nu_{\mathrm{GaAs}} = 0.31$, are cited from Refs. [31,41,42,44] and presented in this work. The surface parameters are chosen from Table 1. The InGaAs and Cr nanofilm surface stresses are $\sigma_s^{\mathrm{InGaAs}} = 1$ N/m and $\sigma_s^{\mathrm{Cr}} = 3$ N/m, respectively. The bulk Young's moduli and Poisson's ratios, $Y_{\mathrm{Cr}} = 109$ GPa, $\nu_{\mathrm{Cr}} = 0.28$, and $Y_{\mathrm{InGaAs}} = 71$ GPa, $\nu_{\mathrm{InGaAs}} = 0.32$, are cited from Ref. [47] and presented from this work. The mismatch strain at interface between InGaAs and Cr is given by $m = 2.03\%$ in Ref. [47] In computational material science, it is still a challenging topic to investigate the alloy surface elastic constants. Therefore, there is no data of GaAs or InAs, but InGaAs surface elastic constant has been found. The surface stress of GaAs and InAs are consistent with typical values of solid surfaces.[31,41,49] For InAGaAs–Cr bilayer systems, the results of surface stress are in good agreement with experimental results, with the surface elasticity ignored. Using Eq. (14a), we can see from Figs. 3 and 4 that the theoretical lines accord well with experimental data.

Tangential elongation deformation is another criterion to explain rolled-up nanotube state. The tangential elongation strain as a thickness function is shown in Fig. 5. Interface mismatch exerts two effects on bilayer system, force (stress) and

torque (moment) effects. Conventionally, the surface stress difference creates a torque on nanofilm and bends it, while surface stress sum generates a force on the nanofilm and expands (or expresses) it. The difference in mechanical property between nanofilm 1 and nanofilm 2 breaks this convention. The difference in surface stress also expands (or expresses) the nanofilm. And surface stress sum also bends nanofilm. Interface mismatch, as well as surface stress, bends nanofilms only along the tangential direction. On the other hand, they expand (or express) the nanofilm not only in the tangential direction but also in the cylindrical direction. The torque effect does not appear owing to the straight property in the cylindrical direction. The cylindrical uniform deformation is also shown in Fig. 5.

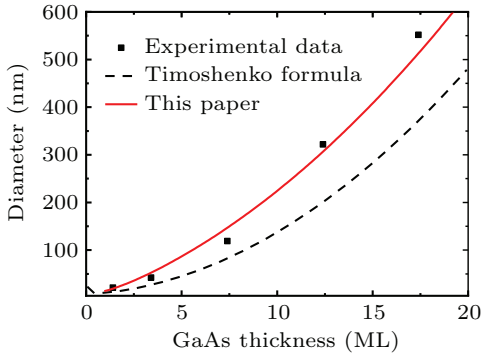


Fig. 3. Curves of diameter of InAs–GaAs tubes versus GaAs layer thickness, with the thickness of InAs layer fixed at 1.4 ML and experimental data cited from Ref. [44].

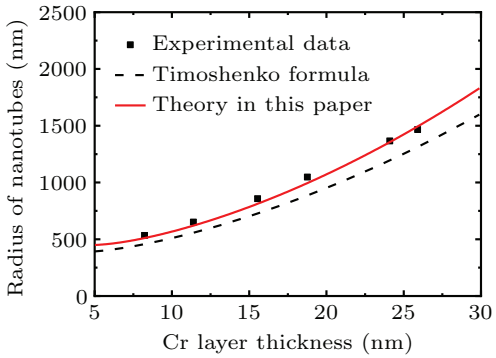


Fig. 4. Curves of radius of InGaAs–Cr tubes versus Cr layer thickness, with the thickness of InGaAs layer fixed at 9.6 nm and the experimental data cited from Ref. [47].

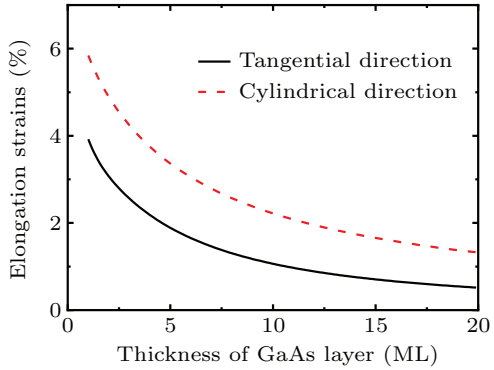


Fig. 5. Tangential elongation strain and cylindrical uniform deformation varying with GaAs thickness.

Cylindrical residual strain affects nanotube diameter and tangential elongation deformation obviously as shown in Figs. 6(a) and 6(b). For the sake of discussion, thickness values of the two nanofilms are chosen as $t_{\mathrm{GaAs}} = 4$ nm, and $t_{\mathrm{InAs}} = 2$ nm, 4 nm, 8 nm, and 16 nm, respectively. Cylindrical direction keeps straight, the uniform residual strain affects nanotube diameter and tangential elongation deformation via Poisson's effect. According to Eq. (14a), the effect of cylindrical strain on diameter is dependent on the difference in Poisson's ratio between two nanofilms, $(\nu_2 - \nu_1)$. If the two nanofilms have the same Poisson's ratio, the effect of cylindrical strain on diameter does not exist. But different nanofilms usually have different Poisson's ratios, especially Poisson's ratio is influenced by surface effect.[32] No mater whether Poisson's ratio is equal to each other, the effect of cylindrical strain on tangential direction elongation deformation always exists. Furthermore, if other parameters are fixed, the rolling curvature and tangential elongation deformation will vary linearly with cylindrical strain. This linear dependence can also be found in Eqs. (14a) and (14b).

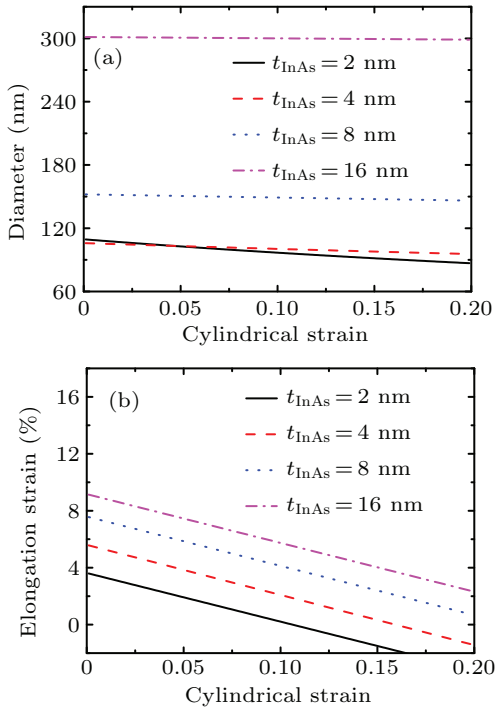


Fig. 6. (a) Nanotube diameter and (b) tangential elongation strain varying with cylindrical strain for different values of thickness t_{InAs}.

The mechanical properties of nanotube are affected by residual strain and stress within nanotube wall. The x-ray microdiffraction analysis demonstrates that the strains within nanotube wall along both tangential direction and radial direction vary linearly with position.[45] In other words, the nanotube wall still holds single crystalline structure. The thickness values of GaAs and InAs sublayers in Fig. 7 are the same as those in Fig. 6. The lattice parameter can be obtained from Eq. (21a). The initial lattice constants of GaAs and InAs nanofilm are $a_{\mathrm{GaAs}} = 0.5650$ nm and $a_{\mathrm{InAs}} = 0.6208$ nm,[31,44]

respectively. Because of rolling behavior, tangential lattice parameter varies linearly in the radial direction. Cylindrical lattice parameter holds constant at any position and is independent of r coordinate owing to its straight state. The lattice parameter in the cylindrical direction is very different from that in the tangential direction. This anisotropic property of lattice parameter is lost in the isotropic Timoshenko formula. Because the coherent lattice parameters, cylindrical lattice parameters, and tangential lattice parameters keep continuous and there is no sudden change at interface. However, the radial lattice parameter behaves sudden change at interface. Initial lattice parameters with no residual strain are different from each other (in the two sub-layers). For different initial lattice parameters, the same lattice parameters in the cylindrical direction and tangential direction, at interface, mean different strains as shown in Figs. 8(a) and 8(b). Different in-plane strains induce different radial strains in the two sub-layers. Therefore, radial lattice parameter undergoes a sudden change at the interface. On the other hand, the difference in Poisson's ratio between two sub-layers also induces the sudden change of radial lattice parameter. Strains along the radial direction and tangential direction are shown in Figs. 8(a) and 8(b). The InAs interface means the InAs sub-layer side near the interface, while GaAs interface refers to the GaAs sub-layer side near the interface. The strains at the InAs interface and GaAs interface follow different laws as shown in Figs. 8(a) and 8(b), which means the sudden change at interface. The tangential strain is composed of elongation strain $\varepsilon_{i,0}$ and bending strain rk as shown in Eq. (1a). For a relatively low thickness of GaAs ($t_{\mathrm{GaAs}} < t_{\mathrm{InAs}}$), the coordinate of GaAs (as well as the interface) is minus, i.e. $r < 0$. With GaAs thickness decreasing, the elongation $\varepsilon_{i,0}$ and bending curvature k increase, but bending strain rk decreases. Therefore, in a relatively low thickness of GaAs, the strain peaks appear in the tangential direction. Radial strain is induced by cylindrical strain and tangential strain. Therefore, the similar strain peaks appear in the radial direction.

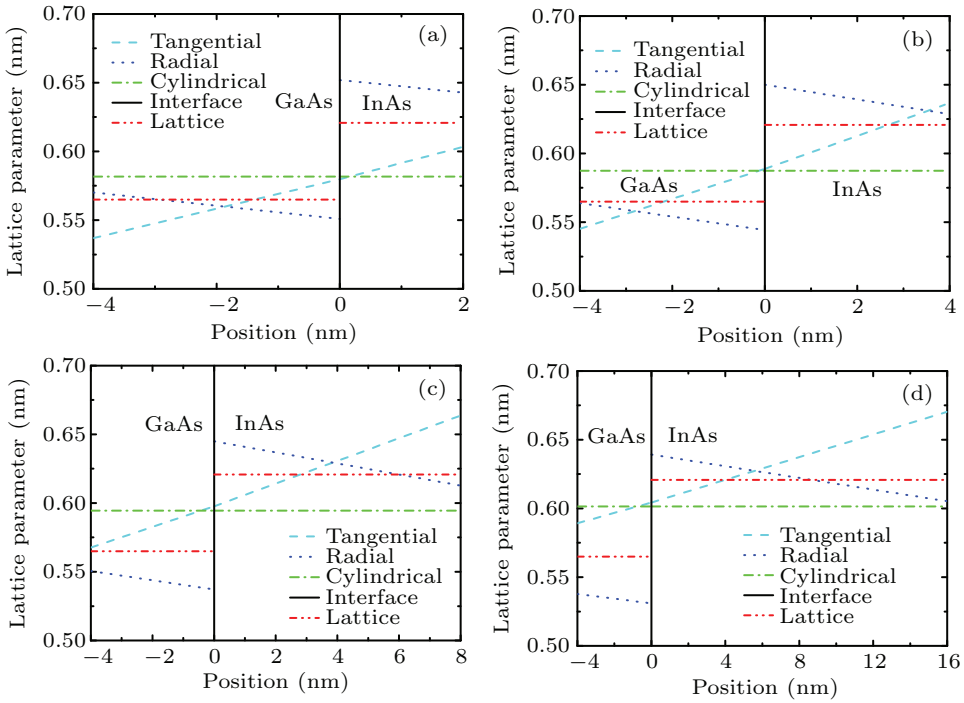


Fig. 7. Lattice parameters within InAs–GaAs nanotube wall versus position at (a) $t_{\mathrm{GaAs}} = 4$ nm and $t_{\mathrm{InAs}} = 2$ nm, (b) $t_{\mathrm{GaAs}} = 4$ nm and $t_{\mathrm{InAs}} = 4$ nm, (c) $t_{\mathrm{GaAs}} = 4$ nm and $t_{\mathrm{InAs}} = 8$ nm, and (d) $t_{\mathrm{GaAs}} = 4$ nm and $t_{\mathrm{InAs}} = 16$ nm.

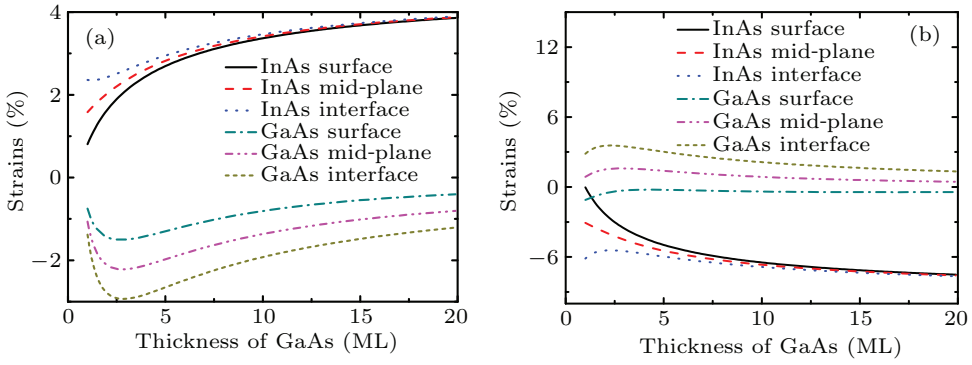


Fig. 8. Residual strains within InAs–GaAs nanotube wall versus thickness of DaAs in (a) radial direction and (b) tangential direction.

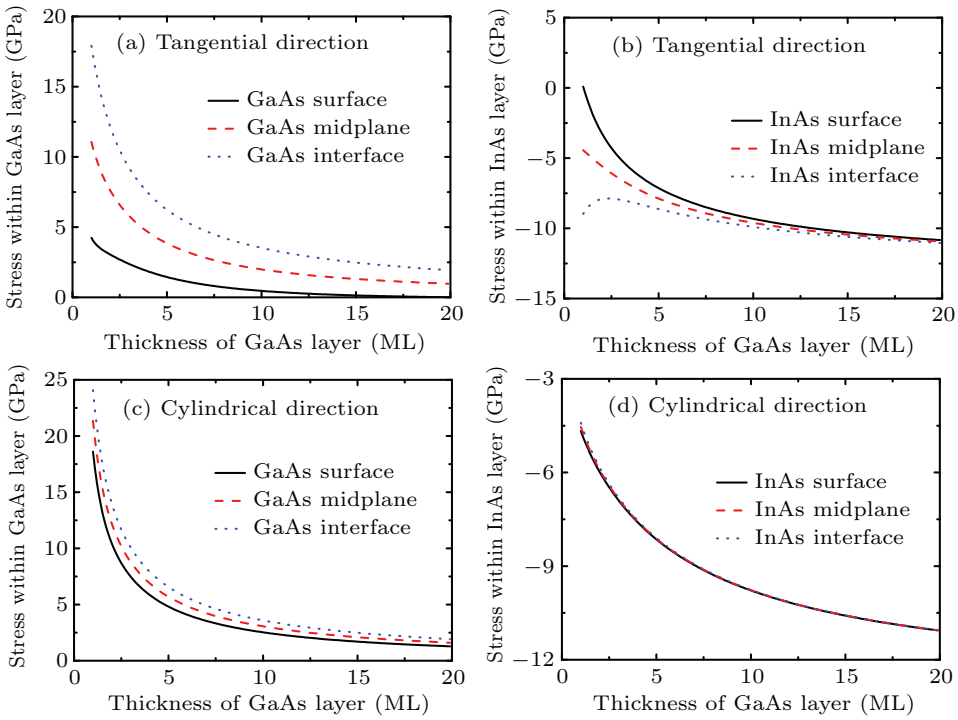


Fig. 9. Residual stresses within InAs–GaAs nanotube wall versus GaAs thickness in (a) GaAs layer along tangential direction, (b) InAs layer along tangential direction, (c) GaAs layer along cylindrical direction, and (d) InAs layer along cylindrical direction.

Owing to full relaxation, radial stress does not exist. The tangential stress and cylindrical stress vary linearly in the radial direction owing to rolling behavior. Tangential stresses are shown in Figs. 9(a) and 9(b). Various tangential strains fail to induce various cylindrical strains owing to the straight shape. Therefore, various residual stresses emerge as shown in Figs. 9(c) and 9(d). The InAs film thickness values in Figs. 9(a)–9(d), are the same as those in Fig. 3. Stresses at InAs interface and GaAs interface follow different laws (not only in the tangential direction but also in the cylindrical direction), which means the sudden change at interface. Residual stress is dependent on residual strain and film elastic constant. Both different residual strains and different elastic constants induce stress to suddenly change at interface. In other words, the sudden change of strain and the different elastic properties between two sub-layers result in the sudden change of stress.

4. Conclusions

In summary, we present a rigorous method of describing the mechanical behavior of rolled-up nanotubes in the framework of continuum theory. The common phenomenon of isotropic bending caused by isotropic mismatch and isotropic surface stress is usually broken by ultrathin nanofilms. Elastic property of nanofilms is influenced by surface elasticity and surface stress. At the same time, symmetry breaking is also of great importance in studying the elastic property of nanofilms. For the formation of rolled-up nanotube, nanoscroll structure affects nanotube radius and tangential elongation deformation via Poisson's effect. Timoshenko formula should be modified anisotropically to explain the mechanical behavior of anisotropic rolling structure of nanotubes accurately. Because of the straight shape in the cylindrical direction, the strain and the lattice parameter are uniform along this direction (except the sudden change of strain at the interface). The various tangential strains induce various cylindrical residual stresses via Poisson's effect, although they are straight along the cylindrical direction.

Acknowledgements

Project supported by the Natural Science Foundation of Shanxi Province, China (Grant No. 201901D111316), the National Natural Science Foundation of China (Grant No. 11874245), the Teaching Reform and Innovation Pproject of Colleges and Universities in Shanxi Province, China (Grant No. J2021508), and the Natural Science Foundation of Inner Mongolia Autonomous Region, China (Grant No. 2020MS06007).

References

[1] Kamto C R T, Sendja B T and Mane J M 2019 *Chin. Phys. B* **28** 093101
[2] Zhuo L C, Liang S H and Zhang T 2015 *Chin. Phys. Lett.* **32** 076401
[3] Ekinci K L and Roukes M L 2005 *Rev. Sci. Instrum.* **76** 061101
[4] Ma J N, Feng L, Wang G F, Lin Z F, Zheng H X and Chen H J 2023 *Chin. Phys. B* **32** 014205
[5] Ma X Y, Zhuang C J, Zeng R and Zhou W D 2021 *J. Phys. D: Appl. Phys.* **54** 105101
[6] Chakraverty S and Behera L 2017 *Chin. Phys. B* **26** 074602
[7] Gireesan S, Torres P, Alvarez F X and Bobbert P A 2020 *Phys. Rev. B* **101** 024307
[8] Dong L, Wei G, Cheng T, Tang J, Ye X B, Hong M Q, Hu L L, Yin R, Zhao S Q, Cai G X, Shi Y, Pan B C, Jiang C Z and Ren F 2020 *ACS Appl. Mater. Interfaces* **12** 8886

[9] Li Y N, Wu P, Zhang S P, Pei Y L, Yang J G, Chen S and Wang L 2022 *Chin. Phys. B* **31** 047203
[10] Fernando R M, David P M, Diego A O, Adolfo D C, José F F and José E G 2019 *ACS Appl. Mater. Interfaces* **11** 13921
[11] Yang Y and Deng Z D 2019 *Appl. Phys. Rev.* **6** 011309
[12] Chen S Y, Yang W D, Song J and Guo F L 2019 *J. Appl. Phys.* **126** 044502
[13] Ye J C, Li J, Chen X H, Huang S M and Ou-Yang W 2019 *Chin. Phys. B* **28** 095202
[14] Pan J N, Qin W Y, Deng W Z and Zhou H L 2019 *Chin. Phys. B* **28** 017701
[15] Khan A N, Ermakov A, Sukhorukov G and Hao Y 2019 *Appl. Phys. Rev.* **6** 041301
[16] Peng J Y, Wang J H, Shen B, Li H L and Sun H M 2019 *Acta Phys. Sin.* **68** 090202 (in Chinese)
[17] Chen C, Song P F, Meng F C, Li X, Liu X Y and Song J 2017 *Nanotechnology* **28** 485302
[18] Celebonovic V, Pesic J, Gajic R, Vasic B and Matkovic A 2019 *J Appl. Phys.* **125** 154301
[19] Izumi S, Hara S, Kumagai T and Sakai S 2004 *Thin Solid Films* **467** 253
[20] Zeng Q and Zhang C L 2018 *Acta Phys. Sin.* **67** 264101 (in Chinese)
[21] Sadeghian H, Yang C K, Goosen J F L, Bossche A, Staufer U, French P J and Keulen F 2010 *J Micromech. Microeng.* **20** 064012
[22] Wang L, Zhang R R and Fang W 2019 *Acta Phys. Sin.* **68** 166101 (in Chinese)
[23] Zhao Y P 2014 *Nano and Mesoscopic Mechanics* (Beijing: Science Press)
[24] Gurtin M E and Murdoch A I 1975 *Ration. Mech. Anal.* **57** 291
[25] Miller R E and Shenoy V B 2000 *Nanotechnology* **11** 139
[26] Chen C Q, Shi Y, Zhang Y S, Zhu J and Yan Y J 2006 *Phys. Rev. Lett.* **96** 075505
[27] Stan G, Ciobanu C V, Parthangal P M and Cook R F 2007 *Nano Lett.* **7** 3691
[28] Li J G, Wang A X, Narsu B, Yun G H, Gao Z X and Liu D P 2019 *Appl. Phys. A* **125** 434
[29] Li J G, Han M Q, Li L F, Gao Z X and Zhang H L 2019 *Sci. Rep.* **9** 16959
[30] Yao H Y, Yun G H, Narsu B and Li J G 2012 *J. Appl. Phys.* **111** 083506
[31] Li J G, Narsu B, Yun G H and Yao H Y 2015 *J. Phys. D: Appl. Phys.* **48** 285301
[32] Li J G, Narsu B, Yun G H, Wang A X and Gao Z X 2018 *Appl. Phys. A* **124** 813
[33] Schmidt O G and Eberl K 2001 *Nature* **410** 168
[34] Zhang Y M and Ionov L 2019 *Eur. Polym. J* **119** 32
[35] Xu C H, Wu X, Huang G S and Mei Y F 2019 *Adv. Mater. Technol.* **4** 1800486
[36] Chen Z, Huang GS, Trase I, Han X M and Mei Y F 2016 *Phys. Rev. Appl.* **5** 017001
[37] Stoney G G 1909 *Proc. R. Soc. Lond. A* **82** 172
[38] Timoshenko S 1925 *J Opt. Soc. Am.* **11** 233
[39] Marcus P M 1996 *Phys. Rev. B* **53** 7460
[40] Huang M H, Rugheimer P, Lagally M G and Liu F 2005 *Phys. Rev. B* **72** 085450
[41] Zang J and Liu F 2008 *Appl. Phys. Lett.* **92** 021905
[42] Grundmann M 2003 *Appl. Phys. Lett.* **83** 2444
[43] Songmuang R, Deneke C and Schmidt O G 2006 *Appl. Phys. Lett.* **89** 223109
[44] Deneke C, Müller C, Jin-Phillipp N Y and Schmidt O G 2002 *Semicond. Sci. Technol.* **17** 1278
[45] Malachias A, Deneke C, Krause B, Mocuta C, Kiravittaya S, Metzger T H and Schmidt O G 2009 *Phys. Rev. B* **79** 035301
[46] Lacheisserie E T 1995 *Phys. Rev. B* **51** 15925
[47] Barcelos I D, Marçal L A B, Deneke Ch, Moura L G, Lacerdaa R G and Malachias A 2016 *RSC Adv.* **6** 103707
[48] Nikishkov G P 2003 *J. Appl. Phys.* **94** 5333
[49] Cammarata R C 1994 *Prog. Surf. Sci.* **46** 1